Synthesis, Crystal Structure of a New Structure Type, and Thermal Analysis of the Ammonium Borophosphate $(NH_4)_2[B_2P_3O_{11}(OH)]$

Katharina Förg[a] and Henning A. Höppe*[a]

Abstract. $(NH_4)_2[B_2P_3O_{11}(OH)]$ was synthesized as a crystalline colorless powder by reaction of $(NH_4)_2HPO_4$, H_3BO_3, and H_3PO_4 under hydrothermal conditions at 180 °C. According to X-ray single-crystal investigations $(NH_4)_2[B_2P_3O_{11}(OH)]$ crystallizes in a new structure type in the orthorhombic space group $P2_12_12_1$ (no. 19) [Z = 4, a = 4.509(3), b = 14.490(11), c = 16.401(12) Å, R_1 = 0.046, wR_2 = 0.093, 1682 data, 200 parameters]. The crystal structure comprises infinite layers of corner-sharing borate, phosphate and hydroxo-phosphate tetrahedra with ammonium ions in-between. The loop-Branched (lB) *zweier*-single layer reveals an open-Branched (oB) *vierer*-single ring as fundamental building unit (FBU), which was observed in $(NH_4)_2Mn^{II}[B_2P_3O_{11}(OH)_2]Cl$[1] for the first time. Besides the spectroscopic properties the thermal behavior is presented as well.

Introduction

Ammonium compounds may act as precursor compounds for materials, e.g. by lowering their synthesis temperature or by providing a certain ratio of elements; moreover, they show crystallographic relations to respective potassium compounds. Recently, we started looking at borophosphates[1] in the context of our systematic investigation of silicate-analogous compounds; typical recent examples are the thiophosphate hydrate $NaMg(PO_3S)\cdot 9H_2O$,[2] strontium fluorophosphates $Sr(PO_3F)\cdot xH_2O$ (x = 0, 1)[3] or borosulfates like $Ba[B_2S_3O_{13}]$ with a layered polymeric anion.[4] Pure ammonium borophosphates are rare and so far only $(NH_4)_2[B_3PO_7(OH)_2]$[5] and $(NH_4)[B_3PO_6(OH)_3]\cdot 0.5H_2O$[6] have been described. The anions of both form borophosphate chains, an ammonium borophosphate with two- or three-dimensional anionic framework structures seems to be unknown so far.

In borophosphate chemistry the FBU (fundamental building unit) represents the essential structural motif, which comprises a certain B:P ratio and furthermore an O:OH ratio (if protonated borophosphates are present).[7] Quite a number of compounds with a B:P ratio of 2:3 is well known.[8–13] Depending on the O:OH ratio and the FBU, the polymeric borophosphate anions form chains or layers. *Ewald* et al. observed that protonated borophosphates with a B:P ratio of 2:3 and an O:OH ratio of 12:1 reveal either layer or chain structures featuring either oB dreier-single rings or olB dreier-single rings, respectively.[13] Reducing the O:OH ratio to 11:2 lead exclusively to the formation of chain borophosphates featuring both mentioned FBUs.[7,9,14] In 2015 we discovered the first layered borophosphate $(NH_4)_2Mn^{II}[B_2P_3O_{11}(OH)_2]Cl$ exhibiting a B:P ratio of 2:3 and an O:OH ratio of 11:2 showing an open-Branched (oB) *vierer*-single ring as novel FBU.[1] $(NH_4)_2[B_2P_3O_{11}(OH)]$ shows a closely related sum formula compared to its already published sister compound $(NH_4)_2Mn^{II}[B_2P_3O_{11}(OH)_2]Cl$. Up to now, all compounds with a B:P ratio of 2:3 had in common a total number of thirteen oxygen atoms, whereas most of them were single or double protonated.

In this contribution we present the first ammonium borophosphate with an anionic layered structure featuring the same FBU as $(NH_4)_2Mn^{II}[B_2P_3O_{11}(OH)_2]Cl$. $(NH_4)_2[B_2P_3O_{11}(OH)]$ (**I**) reveals merely two ammonium ions as cations and thus exhibits for charge compensation an O:OH ratio of 11:1 and in total only twelve oxygen atoms per formula unit.

Results and Discussion

Crystal Structure

$(NH_4)_2[B_2P_3O_{11}(OH)]$ (**I**) crystallizes in a new structure type in the orthorhombic space group $P2_12_12_1$ with four formula units per unit cell. The chirality of the crystal structure was confirmed via SHG experiments. All atoms are located on the general *Wyckoff* position 4*a*. The anionic partial structure of (**I**) consists of infinite layers of corner-sharing borate, phosphate and hydroxo-phosphate tetrahedra (Figure 1 left) avoiding any P–O–P connection; this is in accordance with Pauling's rules and was also observed in $(NH_4)_2Mn^{II}[B_2P_3O_{11}(OH)_2]Cl$[1] and many other borophosphates.[7] The polyanion is constructed by cyclic pentameric $^2_\infty[B_2P_3\Phi_{12}]$ (Φ = O, OH) units comprising a B:P ratio of 2:3. The lB *zweier*-single layer contains an oB *vierer*-single ring as FBU (Figure 1 right), which was observed in $(NH_4)_2Mn^{II}[B_2P_3O_{11}(OH)_2]Cl$[1] for the very first time.

* Prof. Dr. H. A. Höppe
E-Mail: henning@ak-hoeppe.de
[a] Institut für Physik
Universität Augsburg
Universitätsstr. 1
86159 Augsburg, Germany
Supporting information for this article is available on the WWW under **http://dx.doi.org/10.1002/zaac.201700061** or from the author.

Formed by two BO_4 and three $P\Phi_4$ (Φ = O, OH) tetrahedra it can be illustrated with the descriptor 5□:<4□>□.[7,14–16]

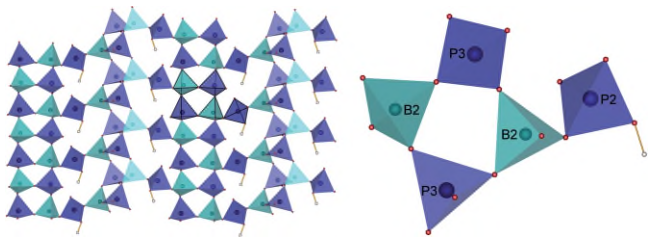

Figure 1. LB *zweier*-single layered anionic partial structure (FBU highlighted) (left) and FBU as oB *vierer*-single ring (right) of $(NH_4)_2[B_2P_3O_{11}(OH)]$; phosphate tetrahedra blue, borate tetrahedra turquoise, and hydrogen atoms white.

Till now all protonated borophosphates with a B:P ratio of 2:3 reveal connection patterns with B–O–B linking in the anionic partial structures as oB dreier-single rings or olB dreier-single rings with exception of $(NH_4)_2Mn^{II}[B_2P_3O_{11}(OH)_2]Cl$.[1] Furthermore, the anionic partial structure always consisted of $[B_2P_3\Phi_{13}]$ (Φ = O, OH) layers or chains, which exhibited an O:OH ratio of 11:2 or 12:1.[1,7] In **I** the O:OH ratio is reduced to 11:1, which has not been observed yet in ammonium borophosphates. Charge compensation leads to the elimination of a hydroxyl group due to the absence of an additional metal cation. Both B and P atoms are coordinated tetrahedrally by either oxygen atoms or hydroxyl groups. B–O bond lengths in the borate tetrahedra range between 1.45 and 1.49 Å, whereas P–O bond lengths in the phosphate tetrahedra lie between 1.48 and 1.56 Å. The bond length P–O_H is 1.53 Å. P–O_{br} (br = bridging) distances range between 1.54 and 1.56 Å, whereas P–O_{term} (term = terminal) distances lie between 1.48 and 1.49 Å. These values correspond to typical data found for other borophosphates.[1,9–11,17] The B–O_{br}–P angles range in a relatively large interval between 106 and 135°, whereas O–B–O and O–P–O angles lie between 103 and 112° (Ø = 110°) and 106 and 115° (Ø = 109°), respectively. Selected bond lengths and angles of **I** are listed in Table 1.

Table 1. Selected interatomic distances /Å and angles /° in $(NH_4)_2[B_2P_3O_{11}(OH)]$.

B–O_{br}	1.450(7)–1.485(7)
P–O_{br}	1.535(4) –1.557(4)
P–O_{term}	1.483(4)–1.487(4)
B–O_{br}–P	105.6(2)–135.3(3)
O–P–O	102.2(1)–115.1(2)
O–B–O	103.4(4)–112.2(4)

We calculated the deviation of the tetrahedra from ideal symmetry employing the method of *Balić-Žunić* and *Makovicky*.[18,19] The five crystallographically different borate, phosphate, and hydroxo-phosphate tetrahedra feature the values –0.36 % (B1), –0.24 % (B2), –0.19 % (P1), –0.32 % (P2), and –0.14 % (P3), which are similar to tetrahedra in other compounds[20–26] and can be classified as regular. The NH_4^+ ions are located between the corrugated borophosphate layers (Figure 2) and form numerous hydrogen bonds (Table S2, Supporting Information).

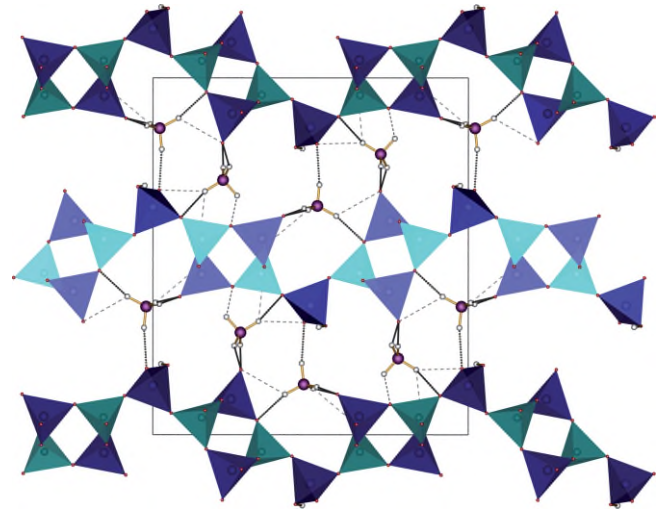

Figure 2. Layered crystal structure viewed along [100]; moderately strong hydrogen bonds shown by dotted thick bonds, weak hydrogen bonds by broken thin bonds; phosphate tetrahedra represented in blue, borate tetrahedra in turquoise, nitrogen atoms violet, hydrogen atoms white.

To prove the phase purity, the reasonability of unit cell parameters and the reflection intensities regarding the possibility of preferential orientation of the crystallites in our sample, a Rietveld refinement based on the structure model of **I** without refining the atomic positions was performed; this led to excellent residuals of R_p = 0.041, R_{wp} = 0.061 and χ^2 = 1.90 (Figure 3 and Table 4).

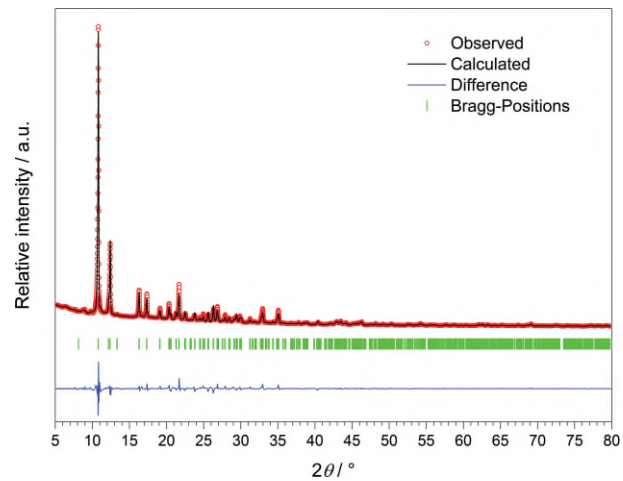

Figure 3. X-ray diffraction pattern and result of Rietveld refinement based on our structure model of $(NH_4)_2[B_2P_3O_{11}(OH)]$ obtained from single-crystal data.

Electrostatic Calculations

The electrostatic consistency of the structure model was proved by calculations based on the MAPLE concept.[27–29] The MAPLE value of the structure model of $(NH_4)_2[B_2P_3O_{11}(OH)]$ deviates by 0.7 % from the sum of MAPLE values of chemically similar compounds. Our crystal

structure model of $(NH_4)_2[B_2P_3O_{11}(OH)]$ thus shows electrostatic consistency, as presented in Table 2.

Table 2. MAPLE calculations for $(NH_4)_2[B_2P_3O_{11}(OH)]$.[25–29]

$(NH_4)_2[B_2P_3O_{11}(OH)]$	$(NH_4)_2HPO_4$[25] + B_2O_3[26] + P_2O_5[27]
MAPLE = 117968 kJ·mol^{-1}	MAPLE = 118780 kJ·mol^{-1}
Δ = 0.7 %	

Infrared Spectroscopy

The infrared spectrum of **I** was recorded between 4000 and 400 cm^{-1} and is shown in Figure 4. The bands at 3344 and 1645 cm^{-1} can be assigned to the stretching and deformation vibrations of the hydroxyl group,[14,17,33–35] whereas vibrations between 3310–2700 cm^{-1} and at 1443 cm^{-1} can be assigned to N–H stretching vibrations.[33,36,37] BO_4 vibrations can be found at 1157, 1126, 901, 879, 569, 534, and 500 cm^{-1}, whereas typical PO_4 vibrations range in the region between 1230 and 400 cm^{-1}. Characteristic bands of symmetric or asymmetric B–O–P stretching and bending vibrations are found at 866 (ν_{as}), 677 (ν_s), 652–638 (δ) and for δ(O–P–O) at 592 cm^{-1}.[38,39]

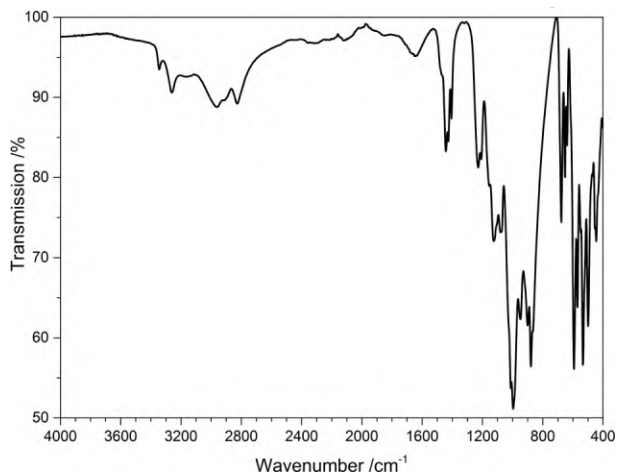

Figure 4. Infrared spectrum of $(NH_4)_2[B_2P_3O_{11}(OH)]$.

Thermal Analysis

The thermal decomposition of $(NH_4)_2[B_2P_3O_{11}(OH)]$ (**I**) was investigated between room temperature and 1400 °C and shows a reasonable stability against thermal treatment up to 300 °C. Below 300 °C, only traces of adhesive humidity lead to a slight weight loss of 1 wt %. The thermogravimetric curve (Figure 5) comprises several steps of mass loss, the total mass loss till 1000 °C amounts to approx. 33 wt %. For a better understanding a temperature-programmed powder X-ray diffraction (TPPXRD, Figure 6) was carried out between room temperature and 950 °C. Temperature fluctuations between the TPPXRD and the TG analysis of ±30 °C may occur due to the slightly different measurement settings. It confirms that the compound is stable up to approximately 330 °C. At higher temperatures the intermediate formation of $NH_4H(PO_3)_2$ (350–500 °C), PON (700–900 °C), and BPO_4 (340–950 °C) is ratified.

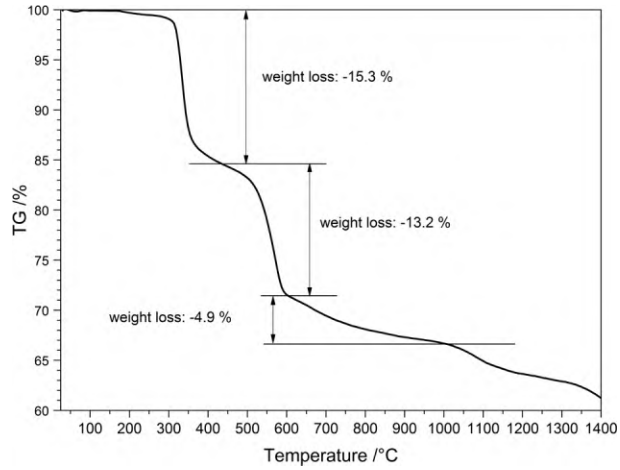

Figure 5. Thermogravimetric analysis of $(NH_4)_2[B_2P_3O_{11}(OH)]$.

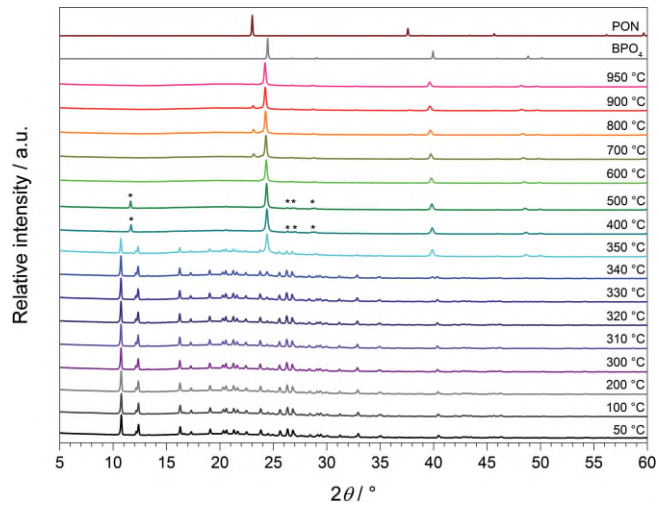

Figure 6. Temperature-programmed powder X-ray diffraction patterns of $(NH_4)_2[B_2P_3O_{11}(OH)]$ recorded between 50 and 950 °C and calculated powder diffraction patterns from single-crystal data of BPO_4[40] (grey) and PON[41] (brown); the reflections of $NH_4H(PO_3)_2$[42] as a further intermediate phase are highlighted with asterices.

Based on the temperature-dependent X-ray powder diffraction the following decomposition equation can be suggested:

$(NH_4)_2[B_2P_3O_{11}(OH)] \rightarrow NH_3 + HBO_2 + 2.5H_2O + 0.5P_2O_5 + PON + BPO_4$ (final product)

The new insights of the TPPXRD study including the corresponding theoretical mass losses are summarized in Table 3.

The comparison with the thermogravimetric curve of $(NH_4)_2[B_2P_3O_{11}(OH)]$ (Figure 5) shows that the observed total mass loss of approx. 39 wt % till 1400 °C fits almost perfectly the sum of the theoretical mass losses calculated based on the TPPXRD results and formation of BPO_4 (38.5 wt %). The first step of mass loss at 350 °C reveals 15.3 wt % (incl. 1 wt % due to humidity) matching well with the theoretical mass loss of one and a half moles of NH_3 and a mole H_2O per (I)

Table 3. Decomposition process during the temperature-dependent X-ray powder diffraction and TG of $(NH_4)_2[B_2P_3O_{11}(OH)]$.

Compound	Temperature range /°C	Calculated mass loss / wt% (experiment)
$2(NH_4)_2[B_2P_3O_{11}(OH)]$ – $(3NH_3 + 2H_2O)$	RT–350 ≥ 350	13.7 (15.3)
$NH_4H(PO_3)_2 + 4BPO_4$ – $(½P_2O_5 + 2.5H_2O)$	350–500 > 500	15.8 (13.2)
$PON + 4BPO_4$ – PON	700–900 >900	9.0 (4.9)
$4BPO_4$	≥ 900	∑ = 38.5 (38.7)

(13.7 wt%) leading to a mixture of $NH_4H(PO_3)_2$ and BPO_4, respectively. Indeed, the synthesis of $NH_4H(PO_3)_2$ is reported to occur around 400 °C, but nothing is mentioned about its decomposition.[42] Also, the second step around 500 °C (13.2 wt%) fits roughly to the theoretical mass losses (15.8 wt%) in this temperature range. After decomposition and loss of PON the final product BPO_4 is obtained. At 950 °C BPO_4 is present as single crystalline phase. With further increasing temperature up to 1400 °C further steadily mass loss is observed, which is due to the continuous evaporation of amorphous residues. According to *Schmidt* et al. BPO_4 is stable up to at least 1100 °C.[40]

Conclusions

In this contribution we demonstrated the phase-pure synthesis and crystal structure determination as well as the spectroscopic and thermal characterization of $(NH_4)_2[B_2P_3O_{11}(OH)]$ as a further representative in the borophosphate family with a B:P ratio of 2:3. In this group it is the first borophosphate with a reduced O:OH ratio of only 11:1. Previously, the oB vierer-single ring as FBU was exclusively found in $(NH_4)_2Mn^{II}[B_2P_3O_{11}(OH)_2]Cl$.[1] In the title compound it forms parallelly corrugated lB *zweier*-single layers with NH_4^+ ions in-between. It is therefore the very first ammonium borophosphate comprising a layered polymeric anion and only the third ammonium borophosphate to date. The absence of an inversion center in the crystal structure was proven by a successful SHG test (more details can be found in the supplement). All bands observed in the IR spectrum could be assigned to the corresponding groups. The electrostatic consistency of the new structure type was confirmed by MAPLE calculations. The layered structure is stable up to 300 °C before $NH_4H(PO_3)_2$ and PON are formed as intermediate decomposition products besides BPO_4 which is the only crystalline phase present above 900 °C.

Experimental Section

Synthesis: $(NH_4)_2[B_2P_3O_{11}(OH)]$ was synthesized under hydrothermal conditions. A mixture of $(NH_4)_2HPO_4$ (792.8 mg, 6.004 mmol, Merck, 99%), H_3BO_3 (247.7 mg, 4.006 mmol, Merck, 99.8%) and H_3PO_4 (0.77 mL, VWR, 85%) was transferred into a 10 mL Teflon autoclave and was kept at 180 °C for 8 d. A colorless suspension was obtained. The product was washed with hot water several times, filtered off, and dried in air overnight. $(NH_4)_2[B_2P_3O_{11}(OH)]$ was obtained as a colorless crystalline powder.

X-ray Powder Diffraction: The homogenized samples were prepared on a stainless steel sample holder and flattened using a glass plate. The measurement was carried out with a Seifert XRD T/T 3003 reflection powder diffractometer at room temperature using Cu-K_α radiation (λ = 1.5418 Å, Meteor 1D linear detector, steps of 0.2°). For the high-temperature measurement the sample was enclosed in a silica-glass Hilgenberg capillary of 0.5 mm outer diameter and investigated between 50–950 °C with a Bruker D8 Advance diffractometer using Cu-K_α radiation (LynxEye 1-D detector, steps of 0.2°, acquisition time 7 s/step, soller slits 2.5°, fixed divergence slit 8 mm, transmission geometry). The generator was driven at 40 kV and 40 mA. The obtained product was phase pure according to X-ray powder diffractometry. The structure model was confirmed and refined by Rietveld analysis[43,44] (Figure 3) using the FullProf program suite and the WINPlotR graphical user interface.[45]

Crystal Structure Analysis: A suited single-crystal was selected for single-crystal X-ray diffraction analysis. Diffraction data were collected with a Bruker D8 Venture diffractometer using Mo-K_α radiation (λ = 0.7093 Å) at a temperature of 298 ± 2 K. The structure was solved by direct methods and refined by full-matrix least-squares technique with the SHELXTL crystallographic software package.[46,47] The N, B, P, and O atoms could be clearly located. Hydrogen atoms

Table 4. Crystal data and structure refinements.

	$(NH_4)_2[B_2P_3O_{11}(OH)]$ (**I**)
Temperature /K	298(2)
Molar weight /g·mol^{-1}	343.62
Crystal system	orthorhombic
Space group	$P2_12_12_1$
a /Å	4.509(3)
b /Å	14.490(11)
c /Å	16.401(12)
V /Å^3	1071.7(14)
Z	4
Calculated density /g·cm^{-3}	2.130
Color	colorless
Dimensions /mm^3	0.018 × 0.026 × 0.102
Absorption coefficient, μ /mm^{-1}	0.626
F(000)	696
Radiation	Mo-K_α (λ = 0.7093 Å)
Diffractometer	Bruker D8 Venture
Absorption correction	multi-scan
Index range (*hkl*)	–5/5; –16/16; –18/18
Theta range (θ_{min}–θ_{max}) /°	2.48–24.00
Reflections collected	14522
Independent reflections	1682
Parameters	200
R_{int}	0.1309
R_1 (all data)	0.0457
wR_2 (all data)	0.0930
Flack parameter x	0.05(17)
Goodness of fit (GooF)	1.037
Residual electron density, Min/max /e$^-$·Å^{-3}	–0.47/0.38
Rietveld refinement:	
a /Å	4.5202(2)
b /Å	14.541(1)
c /Å	16.399(1)
V /Å^3	1077.88(6)
R_p, R_{wp}, χ^2	0.041, 0.061, 1.90

Table 5. Atomic coordinates, Wyckoff symbols, and isotropic displacement parameters U_{eq} /Å^2 in $(NH_4)_2[B_2P_3O_{11}(OH)]$ (O_{br} = bridging oxygen atom; O_{term} = terminal oxygen atom; O_H = oxygen atom of hydroxyl group); standard deviations in brackets.

Atom	Wyckoff symbol	*x*	*y*	*z*	U_{eq}
P1	4*a*	0.1083(3)	0.24777(11)	0.40040(8)	0.0139(4)
P2	4*a*	–0.2579(3)	0.00008(10)	0.36214(9)	0.0160(4)
P3	4*a*	0.3125(3)	–0.15455(10)	0.55036(10)	0.0145(4)
B1	4*a*	0.6029(13)	0.1549(5)	0.4523(4)	0.0153(16)
B2	4*a*	–0.1912(14)	–0.1566(4)	0.4517(4)	0.0149(15)
$O_{br}1$	4*a*	–0.2204(7)	0.2184(2)	0.4028(2)	0.0145(9)
$O_{br}2$	4*a*	0.1562(8)	0.3303(2)	0.4597(2)	0.0164(9)
$O_{br}3$	4*a*	0.2911(7)	0.1659(2)	0.4322(2)	0.0153(9)
$O_{br}4$	4*a*	–0.3112(8)	0.0587(2)	0.4397(2)	0.0174(9)
$O_{br}5$	4*a*	–0.1026(8)	–0.0892(2)	0.3911(2)	0.0153(9)
$O_{br}6$	4*a*	0.4889(8)	–0.1466(3)	0.4702(2)	0.0139(9)
$O_{br}7$	4*a*	0.3633(7)	–0.2529(2)	0.5851(2)	0.0144(9)
$O_{br}8$	4*a*	–0.0191(8)	–0.1456(3)	0.5283(2)	0.0152(9)
$O_{term}1$	4*a*	0.1867(8)	0.2793(2)	0.3171(2)	0.0169(9)
$O_{term}2$	4*a*	–0.5309(8)	–0.0200(3)	0.3144(2)	0.0240(11)
$O_{term}3$	4*a*	0.3891(9)	–0.0856(2)	0.6132(2)	0.0192(10)
O_H1	4*a*	–0.0358(8)	0.0478(3)	0.3051(2)	0.0193(10)
N1	4*a*	0.8881(12)	0.0214(4)	0.6411(4)	0.0263(13)
N2	4*a*	–0.3136(13)	0.2778(4)	0.2137(4)	0.0353(15)
H1	4*a*	0.169(5)	0.026(4)	0.302(4)	0.050
H2	4*a*	0.717(9)	–0.020(4)	0.634(4)	0.050
H3	4*a*	1.079(7)	–0.008(4)	0.630(4)	0.050
H4	4*a*	0.908(15)	0.028(5)	0.7001(10)	0.050
H5	4*a*	0.879(15)	0.081(2)	0.613(3)	0.050
H6	4*a*	–0.136(8)	0.277(5)	0.248(3)	0.050
H7	4*a*	–0.473(10)	0.258(4)	0.251(3)	0.050
H8	4*a*	–0.279(14)	0.233(3)	0.170(3)	0.050
H9	4*a*	–0.304(15)	0.335(2)	0.182(3)	0.050

were added geometrically and were confirmed by MAPLE calculations.[27–29] Relevant crystallographic data and further details of the structure determination are summarized in Table 4. Table 5 and Table S1 (Supporting Information) show positional and displacement parameters for all atoms, respectively.

Further details of the crystal structure investigations may be obtained from the Fachinformationszentrum Karlsruhe, 76344 Eggenstein-Leopoldshafen, Germany (Fax: +49-7247-808-666; E-Mail: crysdata@fiz-karlsruhe.de, http://www.fiz-karlsruhe.de/request for deposited data.html) on quoting the depository number CSD-432664 for $(NH_4)_2[B_2P_3O_{11}(OH)]$ (**I**).

Infrared Spectroscopy: An infrared spectrum was recorded at room temperature with a Bruker EQUINOX 55 FT-IR spectrometer using a Platinum ATR device with a scanning range from 4000 to 400 cm^{-1}.

Thermal Analysis: The thermal analysis was carried out with a Netzsch STA-409 PC thermal analyzer in the temperature range of 22–1400 °C in a nitrogen atmosphere with a heating rate of 5 K·min^{-1}.

Supporting Information (see footnote on the first page of this article): anisotropic displacement parameters of all atoms, overview over reasonable hydrogen bonds and further information on the SHG measurements are given.

Acknowledgements

The authors are grateful to *Prof. Dr. B. Winkler* and *S. Bigalke*, Universität Frankfurt, for performing the SHG experiments.

Keywords: Borophosphate; Ammonium; Boron; Crystal structure; Thermal analysis

References

[1] K. Förg, H. A. Höppe, *Z. Anorg. Allg. Chem.* **2015**, *641*, 1009–1015.
[2] H. A. Höppe, S. Scharinger, J. G. Heck, P. Netzsch, P. Gross, K. Kazmierczak, *Solid State Sci.* **2016**, *62*, 50–55.
[3] S. G. Jantz, L. van Wüllen, A. Fischer, E. Libowitzky, E. J. Baran, M. Weil, H. A. Höppe, *Eur. J. Inorg. Chem.* **2016**, 1121–1128.
[4] P. Gross, A. Kirchhain, H. A. Höppe, *Angew. Chem. Int. Ed.* **2016**, *55*, 4353–4355.
[5] C. Hauf, R. Kniep, *Z. Kristallogr.* **1996**, *211*, 705.
[6] L. Wie, Zh. J. Tai, *Acta Crystallogr., Sect. E* **2007**, *63*, i185.
[7] B. Ewald, Y.-X. Huang, R. Kniep, *Z. Anorg. Allg. Chem.* **2007**, *633*, 1517–1540.
[8] W. Liu, G. M. X. Yang, H. Chen, M. Li, J. Zhao, *Inorg. Chem.* **2004**, *43*, 3910–3914.
[9] B. Ewald, Y. Prots, P. Menezes, S. Natarajan, H. Zhang, R. Kniep, *Inorg. Chem.* **2005**, *44*, 6431–6438.
[10] C. Sevov, *Angew. Chem.* **1996**, *108*, 2814–2816.
[11] H. Engelhardt, W. Schnelle, R. Kniep, *Z. Anorg. Allg. Chem.* **2000**, *626*, 1380–1386.
[12] G.-Y. Yang, S. C. Sevov, *Inorg. Chem.* **2001**, *40*, 2214–2215.
[13] Y.-X. Huang, O. Hochrein, D. Zahn, Y. Prots, H. Borrmann, R. Kniep, *Chem. Eur. J.* **2007**, *13*, 1737–1745.
[14] F. Liebau, *Structural Chemistry of Silicates*, Springer Verlag, Berlin Heidelberg, **1985**.
[15] P. C. Burns, J. D. Grice, F. C. Hawthorne, *Can. Mineral.* **1995**, *33*, 1131–1151.
[16] J. D. Grice, P. C. Burns, F. C. Hawthorne, *Can. Mineral.* **1999**, *37*, 731–762.

[17] T. Yang, J. Ju, F. Liao, J. Sasaki, N. Toyota, J. Lin, *J. Solid State Chem.* **2008**, *181*, 1110–1115.
[18] T. Balić-Žunić, E. Makovicky, *Acta Crystallogr., Sect. B* **1996**, *52*, 78–81.
[19] E. Makovicky, T. Balić-Žunić, *Acta Crystallogr., Sect. B* **1998**, *54*, 766–773.
[20] H. A. Höppe, *J. Solid State Chem.* **2009**, *182*, 1786–1791.
[21] H. A. Höppe, M. Daub, O. Oeckler, *Solid State Sci.* **2009**, *11*, 1484–1488.
[22] H. A. Höppe, K. Kazmierczak, M. Daub, *Z. Anorg. Allg. Chem.* **2010**, *636*, 1106–1110.
[23] H. A. Höppe, K. Kazmierczak, M. Daub, K. Förg, F. Fuchs, *Angew. Chem. Int. Ed.* **2012**, *51*, 6255–6257.
[24] H. A. Höppe, M. Daub, *Z. Kristallogr.* **2012**, *227*, 535–539.
[25] M. Daub, A. J. Lehner, H. A. Höppe, *Dalton Trans.* **2012**, *41*, 12121–12128.
[26] M. Daub, K. Kazmierczak, H. A. Höppe, *Z. Anorg. Allg. Chem.* **2014**, *640*, 46–52.
[27] R. Hoppe, *Angew. Chem. Int. Ed. Engl.* **1966**, *5*, 95–106.
[28] R. Hoppe, *Angew. Chem. Int. Ed. Engl.* **1970**, *9*, 25–34.
[29] R. Hübenthal, *MAPLE*, Program for the Calculation of the Madelung Part of Lattice Energy, University of Gießen, Germany, **1993**.
[30] A. A. Khan, J. P. Roux, W. J. James, *Acta Crystallogr., Sect. B* **1972**, *28*, 2065–2069.
[31] G. E. Gurr, P. W. Montgomery, C. D. Knutson, B. T. Gorres, *Acta Crystallogr., Sect. B* **1970**, *26*, 906–915.
[32] H. Arnold, *Z. Kristallogr.* **1986**, *177*, 139–142.
[33] Y.-X. Huang, G. Schäfer, W. Carrillo-Cabrera, R. Cardoso, W. Schnelle, J.-T. Zhao, R. Kniep, *Chem. Mater.* **2001**, *13*, 4348–4354.
[34] A. Yilmaz, L. Tatar Yildirim, X. Bu, M. Kizilyalli, G. D. Stucky, *Cryst. Res. Technol.* **2005**, *40*, 579–585.
[35] Y.-X. Huang, B. Ewald, W. Schnelle, Y. Prots, R. Kniep, *Inorg. Chem.* **2006**, *45*, 7578–7580.
[36] W. Yang, J. Li, T. Na, J. Xu, L. Wang, J. Yu, R. Xu, *Dalton Trans.* **2011**, *40*, 2549–2554.
[37] H. Shi, Y. Feng, Q. Huang, D. Qiu, M. Li, K. Liu, *CrystEngComm* **2011**, *13*, 7185–7188.
[38] A. Baykal, M. Kizilyalli, R. Kniep, *J. Mater. Sci.* **2000**, *35*, 4621–4626.
[39] A. Baykal, G. Gözel, M. Kizilyalli, R. Kniep, *Turk. J. Chem.* **2000**, *24*, 381–388.
[40] M. Schmidt, B. Ewald, Y. Prots, R. Cardoso-Gil, M. Armbrüster, I. Loa, L. Zhang, Y.-X. Huang, U. Schwarz, R. Kniep, *Z. Anorg. Allg. Chem.* **2004**, *630*, 655–662.
[41] J. M. Léger, J. Haines, C. Chateau, G. Bocquillon, M. W. Schmidt, S. Hull, F. Gorelli, A. Lesauze, R. Marchand, *Phys. Chem. Miner.* **2001**, *28*, 388–398.
[42] K. R. Waerstad, G. H. McClellan, *J. Agric. Food Chem.* **1976**, *24*, 412–416.
[43] H. M. Rietveld, *Acta Crystallogr.* **1967**, *22*, 151–152.
[44] H. M. Rietveld, *J. Appl. Crystallogr.* **1969**, *2*, 65–71.
[45] J. Rodriguez-Carvajal, *Physica B* **1993**, *192*, 55–69.
[46] G. Sheldrick, *SHELXTL*, Version 6.14, Bruker AXS, Karlsruhe, Germany, **2003**.
[47] G. M. Sheldrick, *Acta Crystallogr., Sect. A* **2008**, *64*, 112–122.